Concepts of Airspace Structures and System Analysis for UAS Traffic flows for Urban Areas

Dae-Sung Jang,[*]

KAIST and NASA Ames Research Center, Moffett Field, CA 94035

Corey Ippolito,[†]

NASA Ames Research Center, Moffett Field, CA 94035

Shankar Sankararaman,[‡]

SGT Inc. and NASA Ames Research Center, Moffett Field, CA 94035

Vahram Stepanyan,[§]

University of California Santa Cruz, Santa Cruz, CA 95064

This paper addresses a system centric approach for design and analysis of airspace use in urban unmanned aerial vehicle (UAS) traffic flow control. The approach is based on numerical traffic simulations with a behavioral model of UASs for estimating characteristics of the future UAS air traffic in urban areas and performances of airspace structures. A concept on urban UAS traffic flow control is proposed with various airspace structural designs of different levels of freedom in flight, and a microscopic traffic model of UASs in one of the designs is developed. Fundamental diagrams of simple UAS traffic are obtained and performances of basic airspace structures are compared by using the traffic simulations.

I. Introduction

The rapid technological advance for unmanned aerial systems (UAS) in the last decade enables operations beyond line-of-sight and integration into existing airspaces with enhanced autonomy of the UASs. With the extended capability of UAS technologies, wide-range applicability of UAS is drawing attention to be feasible in the near future.[1–5] Especially, public and commercial needs of UAS operation in urban areas have been increasingly raised.[6–8] However, the environment of operations of UAS in urban areas is highly complex: UASs will operate at a low altitude above/below an uneven skyline in an area with high population density and vigorous ground activities. High-valued ground assets, static obstacles (e.g. wires, poles, buildings, trees), dynamic obstacles (e.g. human, ground vehicles, ships, birds, kites, piloted/manned aerial vehicles), unauthorized UASs, wind gust, and malicious activities (e.g. highjack, jamming, interception) are difficult factors for the UAS operation in dense urban valleys. Thus, as of now, the operation in a populated area is not practicable because of technically challenging aspects, such as robustness in wind gusts, safety assurance against dynamic urban features, and communication/navigation issues.

In a broad view, there can be two approaches handling the technical challenges: vehicle-centric and UAS traffic management[9] (UTM) system-centric approaches. The vehicle-centric approach includes developing on-board components, such as processors, power systems, and sensors, and enhancing the autonomy level of UASs (e.g. decision making, path/mission planning, etc.). On the other side, system-level analysis and development for UTM cover various open research problems: system designs, airspace designs, traffic control/management, navigation/surveillance infrastructures, and communication networks. Through the approaches, it is necessary to identify suitable levels of technologies and requirements of vehicles, sensors, and traffic control systems for the upcoming practical use of UASs in urban areas.

[*]NASA Ames KAIST Postdoctoral Fellow, Intelligent Systems Division, e-mail: daeseong.jang@nasa.gov
[†]Research Scientist, Intelligent Systems Division, e-mail: corey.a.ippolito@nasa.gov
[‡]Research Engineer, Intelligent Systems Division, e-mail: shankar.sankararaman@nasa.gov
[§]Senior Research Scientist, Intelligent Systems Division, NASA Ames Research Center, e-mail: vahram.stepanyan@nasa.gov
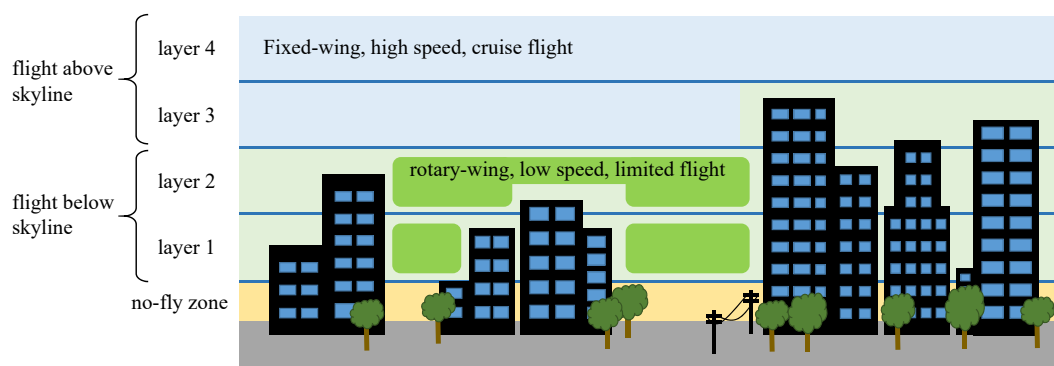
American Institute of Aeronautics and Astronautics

Figure 1. A concept of vertical sectionalization of the airspace in urban areas.

In the system-centric perspective, an agent-based UAS traffic simulation with simplified models can be a practical option for analyzing/validating system designs of traffic control and evaluating their performance without complex computation of building precise UAS models. Various micro-/macro-scopic simulation models have been developed[10–15] in the literature on automobile traffic control systems to emulate collective behavior of human drivers. However, UAS traffic will significantly differ from the automobile traffic due to the additional degree of freedom in vertical motion and fully autonomous behavior of UASs.

Therefore, this paper suggests several different concepts and designs of airspace use for UAS traffic flow control (UTFC) in urban areas, especially focusing on the intersection designs below a skyline of buildings, and presents a microscopic traffic model[a] for numerical simulations in a lane-based airspace structure among the designs. The traffic model is devised with reasonable assumptions on a UAS operating environment and vehicle motions, and is comprised of a separation rule, a vehicle dynamics model, and a behavioral model of vehicles. With the traffic model, two sets of numerical simulations are performed to identify the characteristics of UAS traffic and to compare/analyze the performances of different basic components of the lane-based airspace structure.

II. UTFC System Design in Urban Areas

This section describes a operational concept and assumptions for the overall architecture of an urban UTFC system, which is assumed in this paper. The UTFC system has responsibilities to 1) control/monitor density, throughput, and passage time; 2) supervise/control directional flows of traffic; 3) broadcast traffic situation (e.g. density, passage time, crash, controlled path); 4) detect/track unauthorized flights and warn other vehicles. The design criteria for the UTFC system are listed as follows: assurance of a sufficient level of safety; minimization of infrastructure cost, system complexity, environment effects (e.g. Noise, air pollution, impact on local eco-system), UAS performance requirements, UTFC scope/responsibilities and system requirements, and load for solving traffic flow control problems; maximization of the quality of service (QoS) provided by UTFC; robustness to system failure and scalability with acceptable degradation.

The UTFC system has control over an urban area, where one or several types of airspace structures are designated. Piloted or manned aerial vehicles are segregated from the airspace use at low altitude in the urban area. The airspace in the urban area is divided into several layers by altitude, and sectionalized according to a skyline of buildings (Figure 1). The use of airspaces below and above the skyline is determined by aircraft's maneuverability, speed, and navigation capability. The flight above the skyline is allowed for fixed-wing or high-speed vehicles equipped with navigation devices providing limited usability between high buildings. With a greater speed, the vehicle will be required to be well-equipped with long range sensors and have better separation assurance and collision avoidance capabilities. The vehicles that can slow down to stop and hover arbitrarily can fly below the skyline, as long as functioning navigation systems are provided. Because of restricted spaces between obstacles, more rules are required for the pattern and trajectory of the flight below the skyline than for the ones above the skyline.

---

[a]a microscopic model in traffic simulations is an agent-based model that describes each vehicle's dynamics and individual behavioral rules, whereas a macroscopic model deals with relations of traffic flow variables representing the collective fluid-like behavior of the traffic.
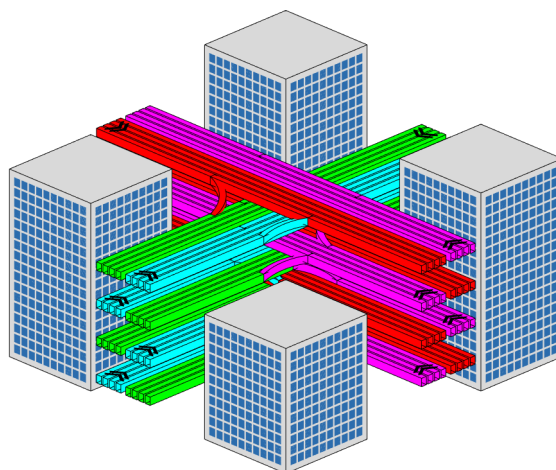
Figure 2. An exemplar composition of airspace structures (sky-lanes) below a skyline.

Table 1. A list of airspace designs

Design	Features
A1	Sky-lanes, coherent lanes, fused crossing
A2	Sky-lanes, coherent lanes, exclusive crossing
A3	Sky-lanes, alternating lanes, exclusive crossing
B1	Sky-tubes, fused crossing with traffic signs
B2	Sky-tubes, fused crossing with transition point control
C	Sky-corridors, transition point control at boundaries

For safety, bulk spaces are reserved around take-off/landing sites, delivery ports, and emergency pullouts. Above each of public areas (e.g. road, park, etc.) and authorized private regions (e.g. rooftop of a civil building), a certain type of airspace structure is designated: details are presented in section III. The UTFC system controls entry/exit of vehicles between these airspaces. A UAS can take-off once receiving permission from the UTFC system, and loiter for a while until the UTFC system approves the UAS's flight plan. Depending on flight rules of a specific airspace structure, where a UAS flies in, flight patterns and a degree of freedom are determined: UAS should follow a certain path in a restrictive structure or has more freedom and responsibility for flight in another one. As the UAS flight plan is executed, UTFC monitors traffic situation and regulates the traffic to enhance QoS. In an off-nominal case, a UAS can make an emergency landing to a ditch point or move to a pullout space. After a flight, UTFC verifies a landing site is clear, and then a UAS requesting for landing can enter the airspace and take a landing procedure.

III.   Designs in Urban Airspace Structures

Airspace above an urban street is sectionalized into multiple layers by altitude, conforming to the terrain. Along the street, each layer is designed to have a certain airspace structure that guides and constrains UAS flights in it. Thus, multi-level (story) networks of the airspace structures are installed in between densely located tall buildings (Figure 2). This section presents three types of design concepts in airspace use: sky-lane, sky-tube, and sky-corridor systems. Each design concept has a different level of freedom for flight trajectory. Sky-lane system is the most restrictive, whereas sky-corridor allows the most free non-collision flights. For sky-lane and sky-tube systems, free sectors or corridors can be placed above low buildings in an area of an uneven skyline to utilize the airspace, not above roads, and link other lanes and tubes through the space. Each design concept has variants that branch according to the configuration of the airspace structures; the design variants are listed in Table 1.

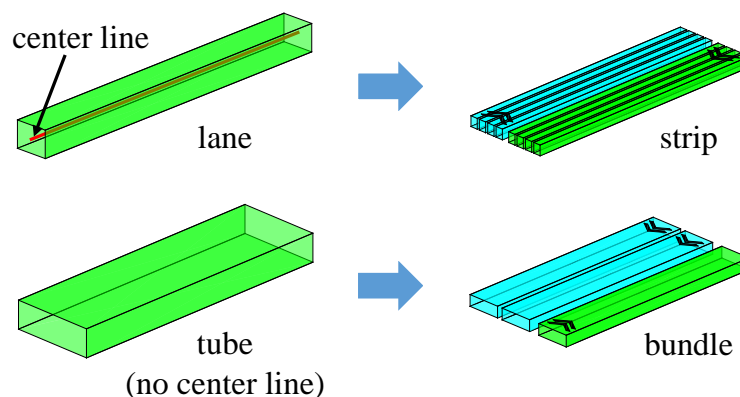American Institute of Aeronautics and Astronautics

Figure 3. Fundamental airspace structures: lanes and tubes constitute a strip and a bundle, respectively. Note that a lane has a reference center line, to which any vehicle should conform in order to fly in the lane, whereas a tube does not have such a constraint. An arrow indicates the direction of traffic flow in each lane/tube.
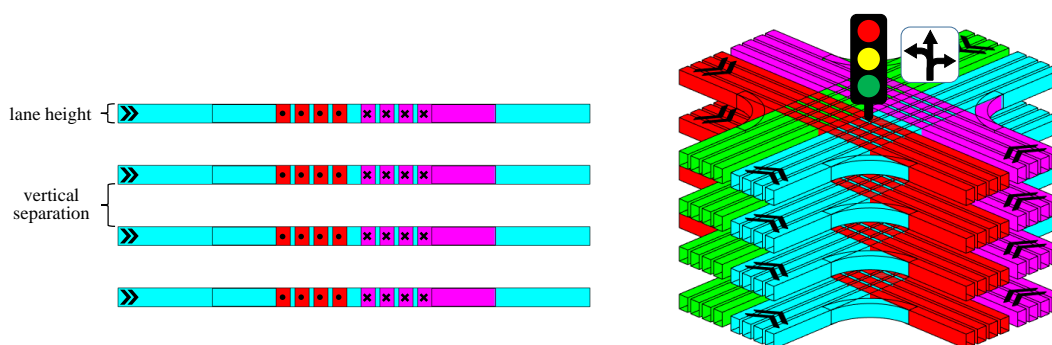

Figure 4. Airspace design A1: a sky-lane system with fused crossings of coherent lanes (right) and its side view (left). Intersecting road strips share the space of the intersection at each layer, and thus a traffic control signal is required

The first design concept is sky-lanes, which represents an extension of a conventional road system into each layer to form a road system in the air with lanes. A lane is a rectangular bar-shaped space extruded from a square that confines the height and width of flight trajectories (Figure 3). Vehicles should follow reference lines placed along the center of lanes in nominal cases, except for changing lanes, turning or escaping in case of emergency, and strongly be requested not to deviate from the lane. Each vehicle in the lane is also responsible for separation assurance between the vehicles ahead/behind of it and collision avoidance of any kinds of obstacles. In a layer, a one-/two-way group of parallel lanes is placed at a level height and constitutes a road strip. Vehicles can change their lanes laterally, and migrate to other layers or crossing strips via left-/right-turns, which are either controlled or free depending on variants of the design concept. In the sky-lane system, the number of lanes in a strip can be adaptive according to traffic situation to regulate/control traffic flows.

The design variants of sky-lane is classified according to lane arrangements and configuration of intersections/interchanges. In the first variant (A1), strips of intersecting roads share the same layer and thus the lanes of the strips are fused at the intersection (see Figure 4). The direction of lanes in a layer can be two-way and the directions of lanes in different layers above the same city street lane are coherent to the direction of the street lane. If there is a space to install a ramp at each corner of an intersection, right turns can be allowed by the ramp. Since incompatible traffic flows share the same space at an intersection, all vehicles follow traffic control in the same manner as ground vehicles. The traffic control service is provided via radio communication by UTFC system infrastructure built at the intersection.

The second (A2) and third (A3) design variants use exclusive stacking of crossed strips, which means no strips above a street intersection share the same layer (see Figures 5 and 6). Therefore, only the half number of strips can be placed than design A1 in the same amount of airspace. Although the utilization of airspace

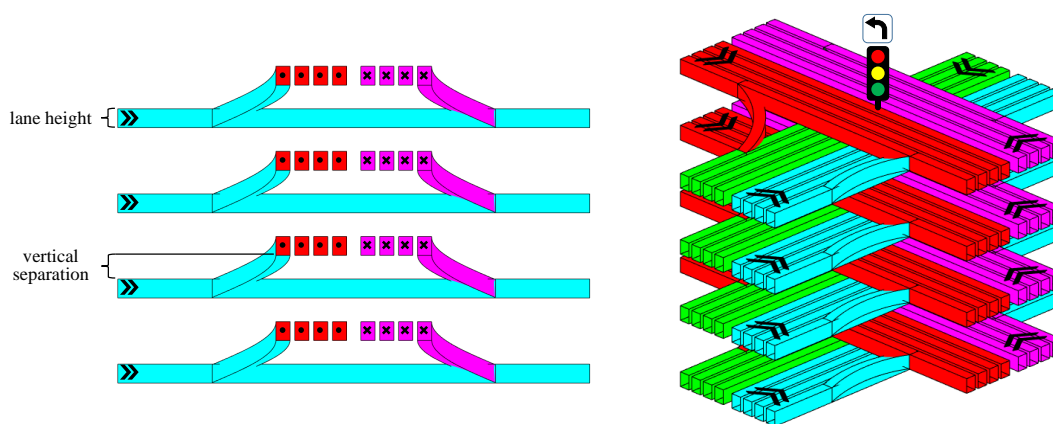American Institute of Aeronautics and Astronautics

Figure 5. Airspace design A2: a sky-lane system with exclusive stacking of coherent lanes (right) and its side view (left). Since all road strips are vertically separated, a double space is required than design A1 for the same number of strips. Left turns may still need a traffic signal.
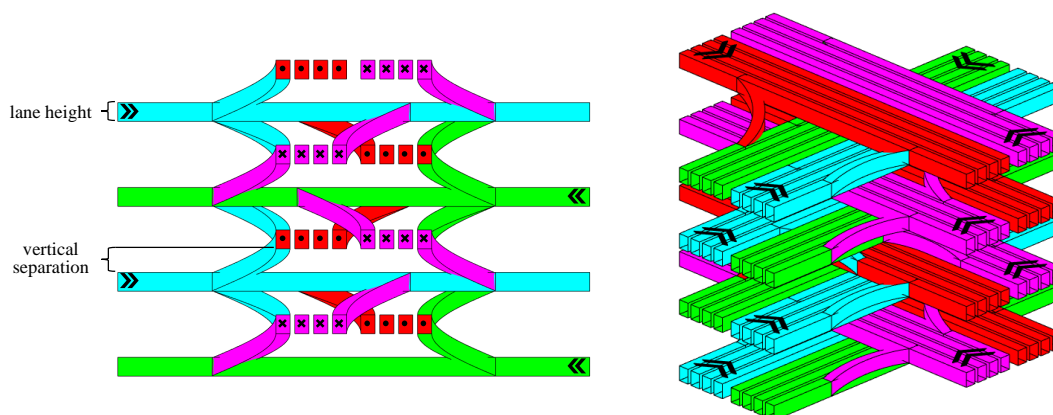

Figure 6. Airspace design A3: a sky-lane system with exclusive stacking of lanes of alternating directions (right) and its side view (left). A double space is required than design A1 for the same number of strips, but this design allows smooth traffic flow with less interruption.

is worsened in the two latter design variants, straight flight along a lane is secured at an interchange, and thus throughput of the system can be enhanced. In both designs A2 and A3, right turns can be allowed by a ramp from the rightmost lane in each strip. The lane directions of different layers are coherent in design A2 (Figure 5), whereas the directions of lanes in neighboring layers alternate in design A3 (Figure 6). Since design A2 imitates a conventional road system into multiple layers in the air, there are reverse-way lanes before entering a crossed lane by using a left turn. Therefore, any non-stop left turns to merge with the traffic stream of the crossed strip are highly limited even though there exist vertical spaces above and below the lane. The left turns in design A2 are only allowed with carefully chosen routes or ordinarily controlled at leftmost lanes as in design A1. On the other hand, smooth paths of left turns into a crossed lane in the lower/upper layer are not obstructed in design A3, since the lanes are placed in an alternating manner (Figure 6). Thus, no active traffic control system is required in design A3 and all-way traffic streams naturally flow down, which minimizes traffic delay.

The second airspace design concept is called sky-tubes. Unlike the sky-lanes, there is no reference line to follow and vehicles can more freely move inside each tube, but should correspond to the traffic direction of the tube. For example, a vehicle can have a lateral speed component but the velocity vector should not deviate greater than a certain angle from the tube's direction. A group of parallel tubes is placed at a level height in each layer, which constitutes a bundle (see Figure 3). The size of the tubes can be adjusted for an adaptive traffic regulation in case of unbalance of two-way traffic. As in the sky-lane system, right turns are allowed if ramps can be placed at the corners of an intersection. However, since a tube is a more bulky

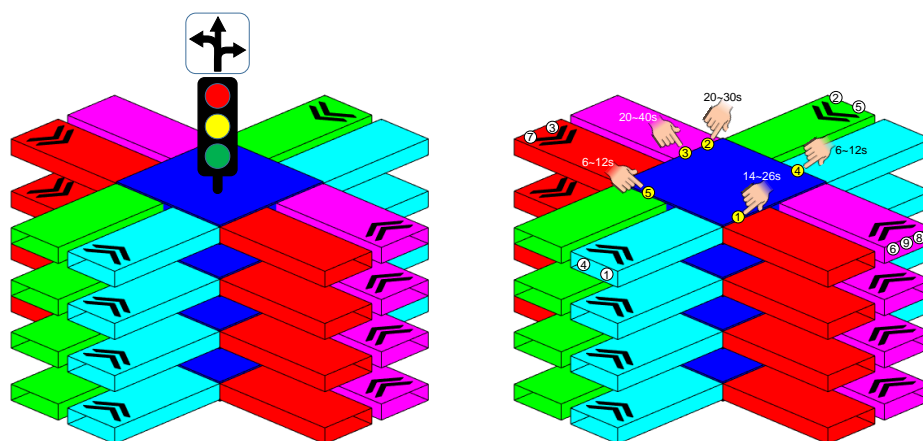American Institute of Aeronautics and Astronautics

Figure 7. Airspace design B1 (left) and B2 (right): sky-tubes of fused crossing. Design B1 uses conventional traffic control at every intersection, and B2 controls traffic by assigning transition points and time windows across intersection boundaries to vehicles.
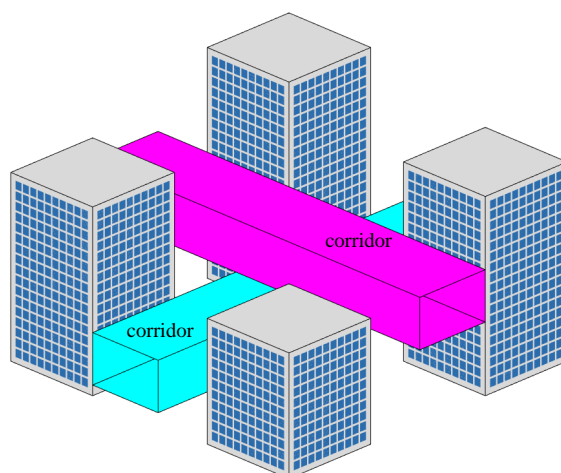

Figure 8. Airspace design C: an exemplar diagram of sky-corridors installed between buildings. UTFC has no control over the flights of vehicles inside a corridor, and it decides only approval/dismissal of vehicles' transition plans between corridors.

airspace structure than a lane and the traffic flow in the tube is not strictly organized, ramps for left turns are not utilized to avoid congestion at the exit to the ramps. Instead, tubes above a street intersection overlap at the same layer and fused at the intersection (see Figure 7).

The sky-tube concept has two design variants in configuration of intersections. The first one (B1) requires a traffic control system at every intersection, and the flight into the fused crossing is totally determined by a UTFC system (Figure 7 (left)). The other design variant (B2) controls the traffic by assigning transition waypoints and time windows of vehicles passing through the boundaries of a fused intersection (Figure 7 (right)). In both designs, separation assurance and collision avoidance among the traffic of more relaxed flights are obligatory for vehicles in either cases of tubes and fused intersections.

The third design concept presented in this paper is sky-corridors. The airspace between buildings and above the lower altitude limit along a street is integrated into a bulk space called a corridor. A single corridor may be placed at each layer or it may collectively cover multiple layers below a skyline. The flight inside a corridor is totally managed by each vehicle and vehicles can freely move inside the corridor in any directions as long as safety is secured. Therefore, vertical separation is not guaranteed by layers anymore, rather it is ensured by vehicles themselves. The corridors basically do not overlap above a street intersection: if the width of one street is larger than the other one and then the corridor above the wider street occupies the intersection area; or for similar sized intersecting streets, one corridor goes down to the other one and they

do not share the same space. The transition of vehicles between two corridors occur at the contact surface of the corridors. Unlike the sky-tube system, a UTFC system does not provide waypoints and time windows, but each vehicle decides its transition plan. The role of the UTFC system for the corridor transition is to determine approval/dismissal of the vehicle's plan and may be to adjust time windows to regulate traffic.

We briefly compare the presented system designs in Table 2. Each of the designs has pros and cons in different perspectives, e.g. space use, simplicity, needs for infrastructure, performance, robustness, and UTFC system's computational load. Communication requirements and information required to be transmitted between UASs, from UTFC to UAS, and UAS to UTFC can also be quite different among the designs.

IV.   Simulation Model in Lane Based Systems

This paper includes UAS traffic simulations with simplified dynamics models of multiple UASs in the lane-based airspace structures (sky-lanes) described in the previous section. Since the simulation environment is built for testing feasibility and performance of the airspace designs, a proper level of abstraction for both of UAS and UTFC systems is required. In the literature on automobile traffic system modeling and intelligent traffic management, various micro-/macro-scopic models have been developed.[10–15] However, the most of the work is of emulating collective phenomena of vehicles by human drivers, which are highly non-linear and sub-optimal. In this paper, it is assumed that UAS systems in near future are intelligent with greater autonomy, and the behaviors of the UASs are considerably different to the ones of human drivers on the ground. This section describes separation assurance in the sky-lane systems and simplified vehicle dynamics for rotary-wing UASs operating below a skyline and behavioral models of following rules in the sky-lane systems.

A.   Separation Assurance

As in air traffic control for manned aircraft, separation assurance in a UTFC system is a critical problem for safe operation. The separation assurance of rotary-wing UASs flying in a sky-lane system has noticeable differences with the one for manned aircraft. Since the separation for manned aircraft is designed for basically commercial fixed wing aircraft, which generate wake along their trajectory, the horizontal separation distance depends on the size of aircraft and resolution of ground sensors and communication systems. On the other hand, rotorcraft wake mainly propagates downward and is not a high-impact issue in operations of multiple UASs at the same altitude, and thus the horizontal separation for rotary-wing UASs has a factor rather similar to the automobile traffic. Also, separation assurance can be carried by highly autonomous vehicles themselves by using their own sensors and communication network whereas monitoring and controlling separation of every UAS in an urban area requires high-cost infrastructure.

In separation assurance of UAS in sky-lane systems, we assume that lateral and vertical separations are given by the designs of airspace structures; vehicles keep level flight along the reference center line of a lane unless they move into neighbor lanes or other altitude layers. The vehicles are safely separated laterally by a lane width and gap between two lanes and vertically by altitude difference of layers. Therefore, the main issue in separation assurance of UASs is longitudinal separation along the lane direction for prevention of collision. This separation is determined by vehicle's speed, maneuverability, and sensor system capability. Though the required separation can be minimized by coordination via communication, e.g. platooning, this paper pursues a conservative policy that the vehicles are sufficiently separated to guarantee their safe operations even with only on-board sensors in case of communication failure.

1.   Longitudinal Separation

Each vehicle in a lane has responsibility of collision avoidance in the direction of flight. Suppose two vehicles, a predecessor and a follower flying right after the former, are cruising in the same lane, and then the follower has the responsibility of collision avoidance. In case that the predecessor suddenly changes its behavior, for instance, it decelerates to stop, the follower must assure a certain safe distance to prevent collision, taking into account maneuverability and responsiveness of itself and the predecessor. Longitudinal separation is the safe distance between two vehicles flying consecutively along the same lane.

Assuming that a vehicle can generate a maximum horizontal force by rotor thrust in a level flight, a distance traveled until the vehicle totally stops with respect to ground, called braking distance, is a factor of determining longitudinal separation. This braking distance is dependent on the maximum thrust, initial

Table 2. Comparison of airspace designs

Airspace concept	Design variant	Advantages	Drawbacks
Sky-lanes	A1: Coherent lanes Fused crossing	Saves space Simple, intuitive Rules of road and traffic control on the ground can be extended	Requires traffic control signals at every crossroad Increases traffic delay Vulnerable to wind gust
	A2: Coherent lanes Exclusive crossing	Simple Reduces complexity of traffic control at crossroads Reduces traffic delay for straight flight	Requires double space Requires a lane change rule and a yield rule at ramps Vulnerable to wind gust
	A3: Alternating lanes Exclusive crossing	No traffic control at crossroads Minimizes traffic delay for straight flight and turns	Requires double space Complex Requires a lane change rule and a yield rule at ramps Vulnerable to wind gust
Sky-tubes	B1: Fused crossing with traffic signs	Saves space Simple, intuitive Flexible flight	Requires rules of road Requires traffic control signals at every crossroad Increases traffic delay
	B2: Fused crossing with transition point control	Saves space Simple Flexible flight	Requires rules of road Requires traffic flow control by setting transition plans May increase traffic delay
Sky-corridors	C: Transition point control at boundaries	Saves space Simple More flexible flight	Requires rules for separation assurance and collision avoidance Requires traffic flow control by setting transition plans May increase traffic delay

American Institute of Aeronautics and Astronautics

vehicle speed and wind speed. Another important factor is a delay time between a change of predecessor's motion and a follower's action, named hereafter reaction delay, and it includes sensor, computation and mechanical delays. During the reaction delay, the follower will remain flying at almost the same speed as the initial one. Therefore, the follower slips for a distance until its maneuvering force for braking becomes effective.

In normal flight in a lane, the major component of motion is in the direction of the lane, and the longitudinal equation of motion of a vehicle under a constant deceleration $a > 0$ from rotor thrust is described as below:

$$\ddot{x} = \begin{cases} -a - k_d(\dot{x} - w_\parallel)^2, & \dot{x} \geq w_\parallel, \\ -a + k_d(\dot{x} - w_\parallel)^2, & \dot{x} < w_\parallel, \end{cases} \tag{1}$$

where x is the vehicle's position along the lane, k_d is a drag coefficient, $w_\parallel$ is the parallel component of wind velocity; the effect of the orthogonal wind component is ignored here. Equation (1) is a pair of Riccati equations, i.e. first order quadratic ordinary differential equations, of the longitudinal velocity of the vehicle $v := \dot{x}$, of which analytic solutions are available (derivations are omitted in this paper). For a headwind case ($w_\parallel < 0$), the brake distance d_{brake} from a initial velocity v_0 to a stop $v = 0$ is:

$$d_{\text{brake}} = \frac{1}{k_d} \ln \frac{\sqrt{k_d a}\, e^{k_d w_\parallel t_{\text{brake}}}}{\sqrt{k_d a}\cos\sqrt{k_d a}\, t_{\text{brake}} + \sqrt{k_d a}\sin\sqrt{k_d a}\, t_{\text{brake}}}, \tag{2}$$

where the time required for braking t_{brake} is:

$$t_{\text{brake}} = \frac{1}{\sqrt{k_d a}} \tan^{-1} \frac{\sqrt{k_d a}\, v_0}{a + k_d w_\parallel^2 - v_0 k_d w_\parallel}. \tag{3}$$

For a tailwind case ($w_\parallel \geq 0$),

$$\begin{aligned} d_{\text{brake}} &= \frac{1}{k_d} \ln \frac{(k_d w_\parallel + \sqrt{k_d a})e^{-\sqrt{k_d a}\, t'} - (k_d w_\parallel - \sqrt{k_d a})e^{\sqrt{k_d a}\, t'}}{2\sqrt{k_d a}\, e^{-k_d w_\parallel t'}} \\ &\quad - \frac{1}{k_d} \ln \cos \tan^{-1}(v_0 - w_\parallel)\sqrt{\frac{k_d}{a}} + \frac{w_\parallel}{\sqrt{k_d a}} \tan^{-1}(v_0 - w_\parallel)\sqrt{\frac{k_d}{a}}, \end{aligned} \tag{4}$$

where the time t' for braking after the vehicle speed reaches $w_\parallel$ is:

$$t' = \frac{1}{2\sqrt{k_d a}} \ln \frac{\sqrt{a} + \sqrt{k_d}\, w_\parallel}{\sqrt{a} - \sqrt{k_d}\, w_\parallel}. \tag{5}$$

In a special case that $w_\parallel = 0$, the brake distance becomes:

$$d_{\text{brake}, w_\parallel = 0} = -\frac{1}{k_d} \ln \cos \tan^{-1} v_0 \sqrt{\frac{k_d}{a}}. \tag{6}$$

A ground vehicle can be suddenly stopped by a crash, but an aerial vehicle will lose its altitude right after an impact that causes instantaneous momentum loss of the vehicle. Thus, it is sufficiently conservative that an aerial vehicle in a lane assures a safe distance for following its predecessor assuming that the predecessor may harshly decelerate without notice but maintaining controllability. Since a follower does not always have precise and accurate information on the capability and state of its predecessor, the braking distance of the predecessor predicted by the follower is calculated by a conservative assumption on the speed and deceleration of the predecessor: for the predecessor's braking distance, $\min(v_{\text{self}}, v_{\text{pred}})$ is used as the initial velocity and $a_{\text{pred}}(> a_{\text{self}})$ is adopted as the deceleration, where v_{self} and a_{self} are the follower's velocity and deceleration, and v_{pred} and a_{pred} are the ones of the predecessor.

The required separation s_{req} for prevention of collision in a lane is defined as a distance for assuring a minimum separation s_{min} after complete braking following after predecessor's drastic braking:

$$\begin{aligned} s_{\text{req}}(v_{\text{self}}, v_{\text{pred}}, a_{\text{self}}, a_{\text{pred}}, w_\parallel, t_{\text{delay}}) &= d_{\text{brake}}(v_{\text{self}}, a_{\text{self}}, w_\parallel) - d_{\text{brake}}(\min(v_{\text{self}}, v_{\text{pred}}), a_{\text{pred}}, w_\parallel) \\ &\quad + s_{\text{min}} + v_{\text{self}} t_{\text{delay}}, \end{aligned} \tag{7}$$

where t_{delay} is the follower's reaction delay.

B.   Vehicle Dynamics Model and Assumptions

Any rotary-wing UAS approved for flight is assumed to have augmented stability with a well designed attitude control system so that its dynamics can be abstracted as being decoupled. Each vehicle is modeled as a point mass and thus the dynamics is simplified as a 2nd order system of translational motions in a three dimensional space. The equation of motion of a vehicle i under wind is:

$$
\begin{aligned}
\ddot{\mathbf{x}}_i &= \frac{1}{m_i}(\mathbf{f}_i + \mathbf{d}_i(\dot{\mathbf{x}} - \mathbf{w}_i)) - [0 \ 0 \ 1]^T g, \\
\dot{\mathbf{f}} &= \frac{\ln 0.05}{t_{\text{delay},m}}(\mathbf{f}_i - \mathbf{u}_i(\mathbf{x}_i, \dot{\mathbf{x}}_i, \mathbf{X}_{-i}, \dot{\mathbf{X}}_{-i}))
\end{aligned}
\tag{8}
$$

where

$$
\sqrt{f_{i,x}^2 + f_{i,y}^2} \le f_{H,\max}, \quad |f_{i,z} - m_i g| \le f_{V,\max};
\tag{9}
$$

$\mathbf{x}_i$ is the position vector of vehicle i; m_i is its mass; g is the gravitational acceleration; $\mathbf{f}_i = [f_{i,x}, f_{i,y}, f_{i,z}]^T$ is the total transitional force of rotor thrust acting on i; $\mathbf{u}_i$ is an input command, which is a function of vehicle's position, velocity and the ones of other vehicles $\mathbf{X}_{-i}$, $\dot{\mathbf{X}}_{-i}$; $\mathbf{d}_i$ is the drag vector applied to i as a function of vehicle's relative velocity with respect to wind; $\mathbf{w}_i$ denotes wind velocity; $t_{\text{delay},m}$ is a 5% settling time of the rotor force to a command value; and the drag model is quadratic to $\dot{\mathbf{x}} - \mathbf{w}_i$. It is assumed that the magnitude of the horizontal input force is bounded by a maximum value $f_{H,\max}$, which equals to the maximum braking deceleration, and the magnitude of the vertical resultant force after gravity compensation is limited by $f_{V,\max}$.

In a free cruise flight without any obstacles, the force $\mathbf{f}_i$ of rotors of a vehicle and the corresponding command $\mathbf{u}_i = \mathbf{f}_i$ is set to compensate the gravity and drag forces. In other cases, $\mathbf{u}_i$ is determined by the self-state and the states of other vehicles. Those states are acquired by on-board sensors and cooperative communication. Since system delays for reacting against environmental changes are critical to collision avoidance and thus safety, we include major factors on the delays in a simplified manner. The sensors' data acquisition/association time, data fusion/filtering and object identification time are expressed in a bundle as a sensor delay $t_{\text{delay},s}$. The computation time for path re-planning and decision making in a vehicle are modeled as a computation delay $t_{\text{delay},c}$. The settling times for servos and attitude changes of the vehicle is incorporated in a 5% settling time between input command $\mathbf{u}_i$ and force $\mathbf{f}_i$, i.e. mechanical delay $t_{\text{delay},m}$. Total system reaction delay is the sum of these delay factors and it is placed between environmental changes and the vehicle reaction, which is determined by the behavioral model of the vehicle.

C.   Behavioral Model of Vehicles

A behavioral model provides rules of actions for vehicles in various situations and flight modes. We use a model that describes actions of intelligent UAS systems operating in a sky-lane system in urban areas. The behavioral model covers basic motions of vehicles for safety (i.e. separation control) and routing actions (e.g. lane change and turn).

1.   Separation Control

Given the longitudinal separation rule in section IV.A.1, each vehicle in a lane tries to keep a separation distance to its predecessor. Among the independent variables of s_{sep}, it is possible to control only v_{self} and a_{self} by each vehicle. To obey the separation rule, an indirect strategy is used: controlling velocity instead of controlling position to keep the separation-speed relation of the rule. Since velocity control leads to a smaller order nonlinear system than a position control scheme, it is easier to stabilize the controller with a constant gain. The goal of the controller is to track the desired value of vehicle velocity for a measured present separation:

$$
\mathbf{u}_{i,H} = m_i k_{v,i}(v_g - v_i),
\tag{10}
$$

where $\mathbf{u}_{i,H}$ denotes the longitudinal input in the lane direction, $k_{v,i}$ is a control gain, v_g is a goal velocity, and v_i is the vehicle's velocity along the lane. The goal velocity is calculated by an inverse function of required separation s_{req}:

$$
v_g = s_{\text{req}}^{-1}(s \mid v_{\text{pred}}, a_{\text{self}}, a_{\text{pred}}, w_{\parallel}, t_{\text{delay}})
\tag{11}
$$

where s denotes the measured separation to the vehicle's predecessor.

2. Lane Change

Since the longitudinal separation is designed to prevent collision between vehicles in the same lane even under communication failure and lateral separation is valid for only vehicles keeping flight along the reference center lines of their lanes, a lane change action must be accompanied by mutual confirmation of vehicles on lane change plans. Thus, a lane change procedure via communication is used in this paper. Suppose that vehicle 0 intends to enter a neighboring lane between two vehicles, vehicle 1 and 2. Then, the procedure of lane change is as follows. 1) Vehicle 0 slows down to a speed lesser than the one of the preceding vehicle 1, and vehicle 0 starts to maintain longitudinal separation distances for the predecessors in both lanes. 2) Vehicle 0 transmits a lane change plan to near vehicles. As vehicle 2 receives the plan, it reduces its speed to assure longitudinal separation to vehicle 0. 3) Vehicle 2 accepts the plan only if it can secure the separation before the planned time when vehicle 0 enters its lane. 4) If vehicles 2 accepts the plan, vehicle 0 executes the plan and vehicle 2 slows down properly. 5) Otherwise, vehicle 0 waits until vehicle 2 sufficiently slows down to secure the separation, and changes the lane after approval from vehicle 2.

A lane change plan of vehicle 0 is derived to have required separation to vehicle 1 after the change is finished in t_{lc}. Vehicle 0 sends the plan if the required separation after deceleration for t_{lc} is smaller than a estimated separation after the deceleration under the assumption that vehicle 1 maintains its speed:

$$s_{10,\text{req},t=t_{lc}} \le v_1 t_{lc} + s_{10} - (d_{\text{brake}}(v_0, a_0) - d_{\text{brake}}(v_0 - a_0 t_{lc}, a_0)), \tag{12}$$

where v_0 and v_1 denote the velocities of vehicle 0 and 1, s_{01} is the present separation between the two vehicles, and a_0 is planned deceleration of vehicle 0. Once the plan is established and transmitted, vehicle 2 can predict the distance to vehicle 0 after t_{lc}, and thus it verifies whether its required separation distance can be archived with maximum braking:

$$s_{02,\text{req},t=t_{lc}} \le v_0 t_{lc} - 0.5 a_0 t_{lc}^2 + s_{02} - (d_{\text{brake}}(v_2, a_{\max}) - d_{\text{brake}}(v_2 - a_{\max} t_{lc}, a_{\max})). \tag{13}$$

If the separation distance cannot be secured in t_{lc}, vehicle 2 first decelerates properly and then accepts the lane change plan.

3. Turning & Exiting Ramp

Since turning motions within an intersection are secured by traffic control, only the turning with ramps is addressed here. A ramp for turning merges two traffic flow and thus the vehicle density in downstream inevitably increases. Therefore, separation distance cannot be secured with the same speed at the merge point in a busy lane and a vehicle in the ramp cannot fly parallel to the lane where it wants to enter waiting new follower's approval. Thus, a turning plan requires to be transmitted in advance as a vehicle enters a ramp or before it, and the vehicle keeps reporting the remaining distance to the merge point of the ramp for determining its predecessor and follower and calculating separation, so that an identified follower in the lane-to-enter has a sufficient time for assuring separation before the vehicle in the ramp reaches the merge point. This can be achieved with two design factors: first, ramp length and speed limit in the ramp is designed in order that a vehicle cannot pass the ramp before its follower in the lane-to-enter assures separation to the merge point; and the vehicle reports a false remaining distance larger than the real one, and thus a vehicle, which is sufficiently far from the merge point can be assigned as the follower.

V.   Fundamental Diagram of UAS Traffic

A fundamental diagram of traffic flow is a graph that visualizes characteristics of traffic flow on a road system and relations of traffic stream variables: flow flux (i.e. throughput), speed, and density. The original fundamental diagram depicts the relation between throughput and density of traffic, but diagrams of throughput versus speed and speed versus density are often drawn together. From these fundamental diagrams, macroscopic behavior of a traffic system is observed and traffic status (e.g. phase and congestion) and capabilities/characteristics of a road system (e.g. capacity and critical velocity/density) are identified. Since UAS traffic in urban areas does not exist yet, fundamental diagrams drawn from numerical simulations of multiple UASs following pre-designed behavioral rules, expected to describe UAS motions under high-level autonomy, can be useful to predict the characteristics of the future traffic system and to derive flight rules and requirements of road systems, vehicles and supporting infrastructure.

(a) Throughput versus speed

(b) Throughput versus density

(c) Speed versus density
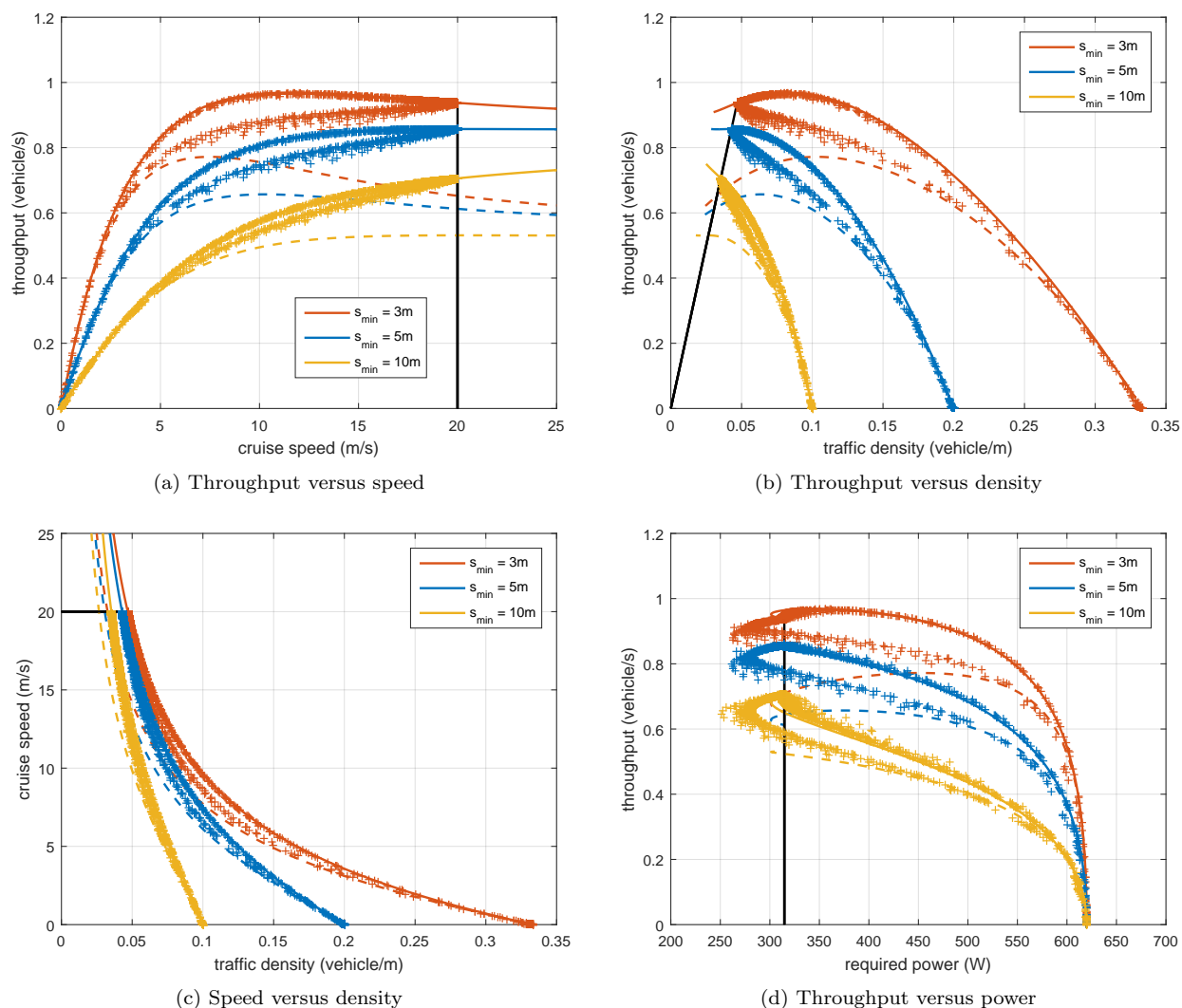
(d) Throughput versus power

Figure 9. Fundamental diagrams of UAS traffic in a single lane: solid lines denote theoretical predictions on traffic of vehicles keeping required separation in equation (7); dashed lines imply the predictions with predecessors that are assumed to stop instantly; black solid lines correspond to a speed limit; and cross marks are time-space averages from traffic simulation results.

In this paper, fundamental diagrams are obtained by testing basic traffic states in a finite flight lane: acceleration from standstill, cruise, and braking to stop. A test simulation scenario includes 20 vehicles successively placed at one end of a 1km lane at the beginning. The initial speeds of the vehicles are zero and the separation distances between them are equal to s_{min}. As a simulation begins, the leader vehicle at the head of the line of vehicles accelerates up to 20m/s, which is the speed limit of this lane, and others follow in order. From the point 50m before the other end of the lane, the leader brakes constantly to stop at the end. The other simulation conditions for fundamental diagrams are as follows: the maximum horizontal acceleration is 8m/s^2; drag coefficient k_d is 0.015m^{-1}; the estimated values of these about each vehicle's predecessor are 16m/s^2 and 0.03m^{-1}; the update rate of a sensor is 10Hz; the communication rate and delay are 10Hz and 0.5s; and system delays are $t_{delay,s} = 0.1$s, $t_{delay,c} = 0$s, $t_{delay,m} = 0.3$s.

Figure 9 shows fundamental diagrams for the traffic in the test simulations with three different minimum separation s_{min}=3m, 5m, 10m: from its subgraph (a) to (d), throughput-speed, throughput-density, speed-density, and throughput-required power relations are presented (the estimation method of required power is described in the following paragraph). In each diagram, solid lines are derived by theoretical predictions when every vehicle keeps the required separation of equation (7) at all cruise speeds, and dashed lines imply

American Institute of Aeronautics and Astronautics

the predictions when each vehicle assumes its predecessor can stop instantly, which means the predecessor's deceleration is infinite. Each black solid line corresponds to the speed limit of the lane. The data points, marked as crosses, are obtained by taking time-space averages from the simulation results. The averaged simulation results well match with the theoretical predictions in the cruise case (solid lines) when vehicle are accelerating, since a conservative assumption on the predecessor's speed is used to calculate the predecessor's braking distance (refer section IV.A.1), and thus the greater speed of the predecessor is not taken into account for calculating separation. However, after the speeds of vehicles reach the speed limit, 20m/s, the vehicles decelerate, and then the averaged results are detached from solid lines and approach to dashed lines. This is because the predecessor of each vehicle always has smaller speed during braking phase, and the required separation is reduced than the one in cruise flight, where a predecessor and a follower have the same speed. From the three basic fundamental diagrams, exhibiting the relation between throughput, speed, and density, we can predict a system performance (throughput) and other traffic flow variables of the lane system with different design parameters and vehicle speeds.

The additional diagram in Figure 9d shows the relation between the throughput of the lane and the required power for vehicle flights. Since minimizing power consumption is a crucial problem for both UTFC systems and UAS operators, this diagram provides considerably important information for design decisions. The required power here is a rate of work that needs to be done on the fluid by rotor systems of a vehicle. This power is estimated by using the Glauert theory[16] in foward flight of rotorcraft with records of vehicle motions in the test simulations. Based on the momentum and energy conservation laws applied in a simple flow model through a rotor disk, the Glauert theory estimates the power provided on the fluid P as below:

$$P = T(v_{\text{ind}} + v_{\|,\infty}), \tag{14}$$

where T is the thrust generated by the rotor, $v_{\|,\infty}$ is the component of relative wind velocity v_∞ parallel to the rotor axis, and v_{ind} is an induced velocity, which is a solution of a quartic equation:

$$v_{\text{ind}}^4 + 2v_{\|,\infty}v_{\text{ind}}^3 + v_\infty^2 v_{\text{ind}}^2 - (T/2\rho A)^2 = 0, \tag{15}$$

where ρ is the density of air and A is the rotor disk area; $\rho = 1.225\text{kg/m}^3$ and $A = 1\text{m}^2$ are used in the simulation. The relative wind velocity is given by the simulation results and the thrust vector is calculated by using vehicle acceleration and drag, and then the parallel wind component $v_{\|,\infty}$ can be computed with the thrust vector. By the Glauert theory, it is predicted that the required power is reduced under upwind to rotor disk. In Figure 9d, after vehicles reach the speed limit, and before the data points get near to dashed lines as vehicles slow down below 5m/s, the required power is considerably reduced than theoretical prediction. Since a vehicle pitches up in order to create decelerating force for braking, upwind appears to the rotor disks of the vehicle and it reduces required power than for cruise flight. This benefit is larger when wind speed is greater at the initial stage of braking.

VI.   Comparative Traffic Simulation

For comparison of performances of different designs of the sky-lane system presented in this paper, UAS traffic at a simple intersection or interchange of two crossing road strips is examined by numerical simulations. Though the designs incorporate multiple layers and complex three dimensional ramps, only a basic structural component vertically repeated in each design is used in this paper, and two of the basic structures reflecting core features of the designs are comparatively analyzed: two intersecting strips sharing space at the same layer (in design A1) and exclusive stacking of two crossed strips (in design A2/A3). Both of the basic structures have two strips crossing at an intersection/interchange and four right-turn ramps. In the intersecting strips, traffic is controlled by a traffic signal, whereas free flow is promoted in the exclusively stacked strips.

In the simulation setting, each road strip is 500m in length and consists of four lanes with two lanes for each way. Every right most lane among one-way lanes has a right-turn ramp of 90m in length to the right most lane of the crossing strip. The recommended speed for reduction of power consumption is assumed to be 18m/s in all lanes and ramps, and thus vehicles maintain this speed if possible. The speed limit is 20m/s in all cases and all other parameters are the same as in section V. At the beginning of a simulation, vehicles flying at the recommended speed with corresponding separation fully occupy the road strips. During the simulation, succeeding vehicles will arrive at the end of each lane with the recommended speed, but if the

American Institute of Aeronautics and Astronautics

(a) Averaged speed variation over time

(b) Averaged density variation over time

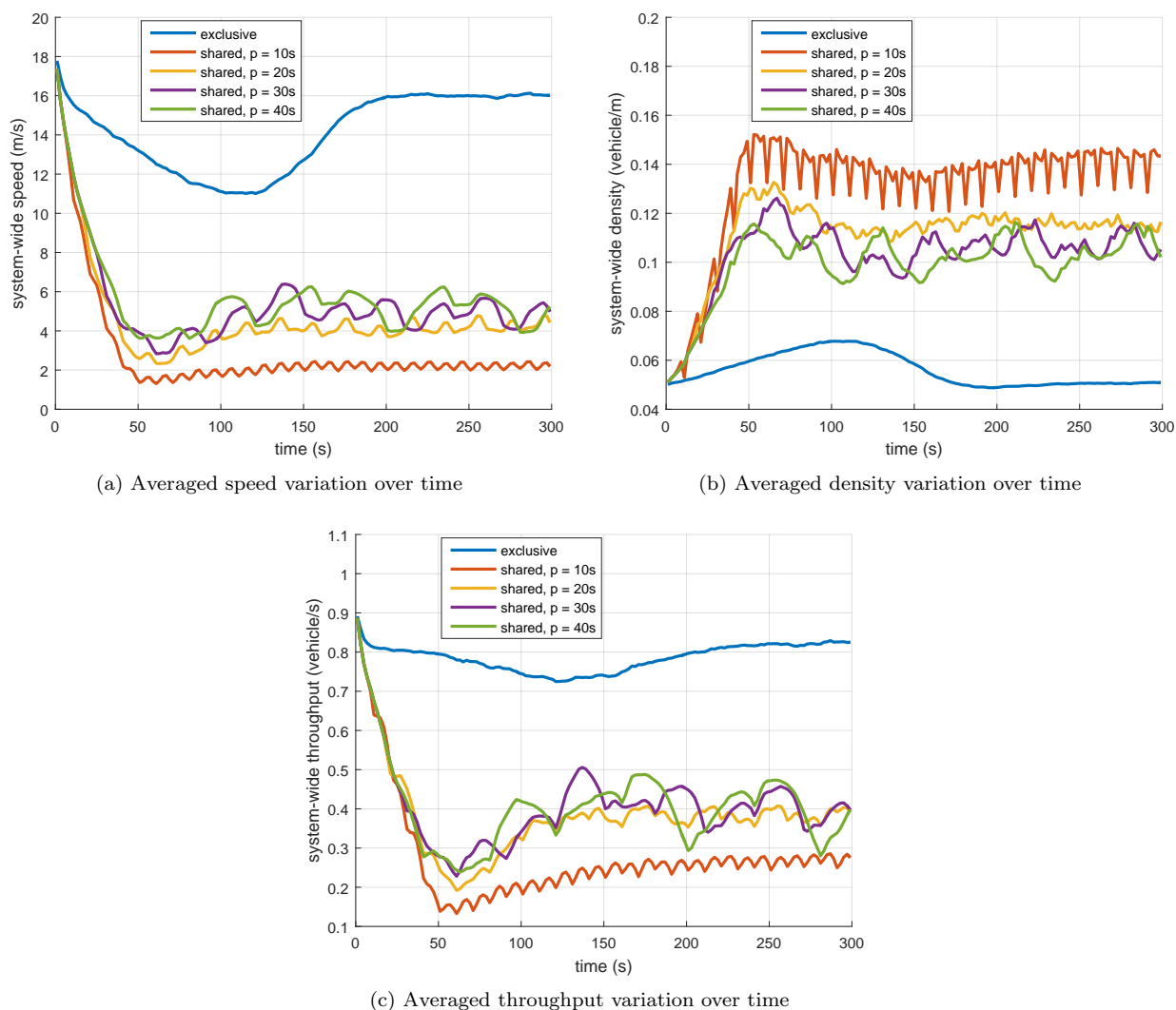(c) Averaged throughput variation over time

Figure 10. Comparative traffic simulation results: each subgraph depicts system-wide averaged speed (a), density (b), and throughput (c) of two crossing road strips; the results of exclusively stacked strips (blue) and intersecting strips of a shared layer with four different traffic control periods (p =10s: red, 20s: yellow, 30s: purple, 40s: green) are included.

separation to their predecessors cannot be assured with the recommended speed, they will appear having a decreased speed that matches with actual separation. Randomly selected 25% of vehicles change its lane during flight in a structure and 25% of vehicles approaching at each ramp will enter the ramp.

Figure 10 depicts averaged traffic simulation results of the two basic structures: averaged speed, density and throughput of vehicles over all lanes of each structure are plotted over time, and the results of 30 random simulation instances are averaged for each curve. For the intersecting strips, four periods of the traffic control signal at the intersection are tested: 10s, 20s, 30s, and 40s. Since intersecting strips share the intersection space and vehicles in two road strips are alternately regulated to stop by the traffic signal, vehicles waiting before the intersection increase traffic density and reduce the throughput of the structure. This traffic delay is alleviated with larger control periods of 20s to 40s, because the effects of time for acceleration and reaction delay accumulated through succeeding vehicles become relatively small. The traffic in the exclusive strips, on the contrary, flows more freely with less interruption, by lane changes and ramp turns, and thus the system-wide throughput is maintained around 0.8 vehicles per second, which is roughly double the results in intersecting strips. However, it should be noted that the exclusive strips require twice the vertical space of the intersecting strips. Therefore, it is expected that for the two systems each of which is built by one

American Institute of Aeronautics and Astronautics

of the two basic structures, the performances in term of throughput are comparable, yet the system of the intersecting strips requires certain infrastructure for traffic control.

VII.   Conclusion

This paper has presented concepts and designs of airspace use for UTFC in urban areas and a microscopic model for traffic simulations in a lane-based airspace structure, which is an extension of conventional road systems. Since there have never existed an urban UTFC system and thus of course UAS traffic, the overall architecture and operational concepts of a UTFC system has been assumed, and under the architecture, multiple airspace structures have been proposed for mainly rotary-wing UAS flights below building heights. Separation assurance, simplified dynamics with quadratic drag and system delays, lane change and turning behavior of vehicles are contained in the microscopic traffic model. By fundamental diagrams and comparative numerical simulations using the traffic model, the characteristics of UAS traffic and performances of basic components of the lane-based airspace structure have been experimentally identified.

Acknowledgments

References

[1]Canis, B., "Unmanned aircraft systems (UAS): Commercial outlook for a new industry," Tech. rep., Congressional Research Service, 2015.

[2]Cox, T. H., Nagy, C. J., Skoog, M. A., Somers, I. A., and Warner, R., "Civil UAV capability assessment," Tech. rep., NASA, 2004.

[3]Gupta, S. G., Ghonge, M. M., and Jawandhiya, P., "Review of unmanned aircraft system (UAS)," *technology*, Vol. 2, No. 4, 2013.

[4]Hockmuth, C. M., "UAVs-the next generation," *Air Force Magazine*, Vol. 90, No. 2, 2007, pp. 70.

[5]Tomić, T., Schmid, K., Lutz, P., Dömel, A., Kassecker, M., Mair, E., Grixa, I. L., Ruess, F., Suppa, M., and Burschka, D., "Toward a fully autonomous UAV: Research platform for indoor and outdoor urban search and rescue," *Robotics & Automation Magazine, IEEE*, Vol. 19, No. 3, 2012, pp. 46–56.

[6]Atkins, E., Khalsa, A., and Groden, M., "Commercial low-altitude UAS operations in population centers," *ATIO Conference*, 2009.

[7]Heutger, M. and Kückelhaus, M., "Unmanned aerial vehicles in logistics: A DHL perspective on implications and use for the logistics industry," Tech. rep., DHL Trend Research, 2014.

[8]Kopardekar, P. H., "Unmanned aerial system (UAS) traffic management (UTM): Enabling low-altitude airspace and UAS operations," Tech. rep., NASA, 2014.

[9]Kopardekar, P., Rios, J., Prevot, T., Johnson, M., Jung, J., and John E III, R., "Unmanned aircraft system traffic management (UTM) concept of operations," *16th AIAA Aviation Technology, Integration, and Operations Conference, AIAA AVIATION Forum*, 2016.

[10]Barceló, J., Codina, E., Casas, J., Ferrer, J., and García, D., "Microscopic traffic simulation: A tool for the design, analysis and evaluation of intelligent transport systems," *Journal of Intelligent and Robotic Systems*, Vol. 41, No. 2-3, 2005, pp. 173–203.

[11]Baskar, L. D., De Schutter, B., Hellendoorn, J., and Papp, Z., "Traffic control and intelligent vehicle highway systems: a survey," *Intelligent Transport Systems, IET*, Vol. 5, No. 1, 2011, pp. 38–52.

[12]Helbing, D., Hennecke, A., Shvetsov, V., and Treiber, M., "Micro-and macro-simulation of freeway traffic," *Mathematical and computer modelling*, Vol. 35, No. 5, 2002, pp. 517–547.

[13]Ng, K. M., Reaz, M. B. I., and Ali, M. A. M., "A review on the applications of Petri nets in modeling, analysis, and control of urban traffic," *Intelligent Transportation Systems, IEEE Transactions on*, Vol. 14, No. 2, 2013, pp. 858–870.

[14]Rahman, M., Chowdhury, M., Xie, Y., and He, Y., "Review of microscopic lane-changing models and future research opportunities," *Intelligent Transportation Systems, IEEE Transactions on*, Vol. 14, No. 4, 2013, pp. 1942–1956.

[15]Roncoli, C., Papageorgiou, M., and Papamichail, I., "Traffic flow optimisation in presence of vehicle automation and communication systems–Part I: A first-order multi-lane model for motorway traffic," *Transportation Research Part C: Emerging Technologies*, Vol. 57, 2015, pp. 241–259.

[16]Leishman, G. J., *Principles of Helicopter Aerodynamics*, Cambridge University Press, 2nd ed., 2006.